Sudden changes in chaotic attractors and transient basins in a model for rattling in gearboxes

Silvio L.T. de Souza [a,*], Iberê L. Caldas [a], Ricardo L. Viana [b], José M. Balthazar [c]

[a] *Instituto de Física, Universidade de São Paulo, CP 66318, 05315-970 São Paulo, SP, Brazil*
[b] *Departamento de Física, Universidade Federal do Paraná, 81531-990 Curitiba, PR, Brazil*
[c] *Departamento de Estatística, Matemática Aplicada e Computacional, Instituto de Geociências e Ciências Exatas, Universidade Estadual Paulista, 13500-230 Rio Claro, SP, Brazil*

Abstract

We consider a model for rattling in single-stage gearbox systems with some backlash consisting of two wheels with a sinusoidal driving. The equations of motions are analytically integrated between two impacts of the gear teeth. Just after each impact, a mapping is used to obtain the dynamical variables. We have observed a rich dynamical behavior in such system, by varying its control parameters, and we focus on intermittent switching between laminar oscillations and chaotic bursting, as well as crises, which are sudden changes in the chaotic behavior. The corresponding transient basins in phase space are found to be riddled-like, with a highly interwoven fractal structure.
© 2004 Elsevier Ltd. All rights reserved.

1. Introduction

Vibro-impact mechanical systems, for which the oscillating parts are subjected to collisions with other vibrating components or rigid walls, is one of the most intensively studied themes in nonlinear dynamics applied to engineering problems [1,2]. Since the considered oscillations do not satisfy the usual smoothness assumptions, classical mathematical methods are applicable only to a limited extent and require extensions both for analytical and numerical methods [3–5]. These impacts can be desirable and even necessary to the operation of some engineering systems, like vibration hammers, driving machinery, milling, impact print hammers, and shock absorbers [6]. On the other hand, there are highly undesirable effects coming from vibro-impact systems like gearboxes, bearings, and fuel elements in nuclear reactors: large amplitude response leading to material fatigue, and high environmental noise due to rattling.

The latter turned to be one of the most important vibro-impact problems, an extensive literature being available on the subject [7–11]. Gear units have typically backlashes, or variable clearances between adjacent moving parts. These backlashes are actually needed to accommodate thermal expansion during the operation of the gearbox system, as well as to allow proper lubrification of the moving wheels. Due to these backlashes, the gear teeth may lose contact for a short period of time and eventually collide again producing a hammering effect and high dynamical overloads [7,8]. This effect has been observed to occur, for example, in small power plants [6].

---

* Corresponding author.
E-mail address: thomaz@if.usp.br (S.L.T. de Souza).

Other context where gear-rattling has been described is in spur gears of engines driving the camshafts and the injection pump shafts [8]. In change-over gears of automobiles, for example, rattling is the source of discomfortable noise. Pfeiffer and collaborators have studied these and related gear-rattling problems by considering theoretical models comprising of two spur gears with different diameters and a gap between the teeth (single-stage rattling) [7,8,12]. The motion of one gear is supposed to be given, whereas the motion of the other gear results from the vibro-impact dynamics of the system [12]. Many analyses have focused on the case for which the driving wheel undergoes a sinusoidal motion with well-defined amplitude and frequency [8].

Numerical studies have shown a rich dynamical behavior for the problem, as coexisting periodic and chaotic attractors, with fractal basins of attraction [13,14]. Control of chaotic dynamics is also possible by means of stabilizing unstable periodic orbits embedded in the chaotic attractor [15]. The above mentioned models often assume the external driving to come from an ideal source, such that its motion is not affected by the gear response. Nonideal systems, for which the driving source has a limited power-supply, are also interesting from the gear rattling point of view [16].

In this paper we aim to explore some dynamical features hitherto not fully explored in the gear-rattling model of Pfeiffer and collaborators [7,8,12], with emphasis on sudden changes in the chaotic attractors which can occur through crisis and intermittency mechanisms. The observable consequence of the occurrence of crisis is the emergence of a chaotic transient which resembles at first the dynamics of the chaotic attractor, and eventually escapes to another attractor, or else asymptotes to infinity [17].

This paper is organized as follows: Section 2 presents the basic equations governing the gear-rattling model we are investigating and comment on the hypotheses underlying this derivation. Section 3 shows some numerical evidences of crisis and intermittency in the chaotic dynamics of the problem. Section 4 present numerical results of the post-critical scenario, showing the existence of riddled-like transient basins, which are characterized by extreme final state sensitivity. Our conclusions are left to the last section.

2. Basic equations

In the gear-rattling model proposed by Pfeiffer [7,12], a single-stage gearbox system is represented by two gears with radii R and R_e, and with a backlash v between the teeth (Fig. 1). The motion of the driving wheel is supposed to be a harmonic oscillation, whereas the second gear has its dynamics resulting from the repeated impacts between the two teeth. Between the impacts, the motion of the second wheel is governed by a linear differential equation and can be analytically determined. The impacts are treated by modifying the initial conditions of the motion, according to Newton's law of impact [18].

Let φ be the angular displacement of the second gear in the absolute coordinate system. The rotation dynamics is governed by the following equation of motion [7,8,12,18].

$$m\varphi'' + d\varphi' = -T, \tag{1}$$

where m, d and T are the moment of inertia, the damping coefficient, and the external torque due to the impacts caused by the backlash between the teeth. The primes denote differentiation with respect to time.
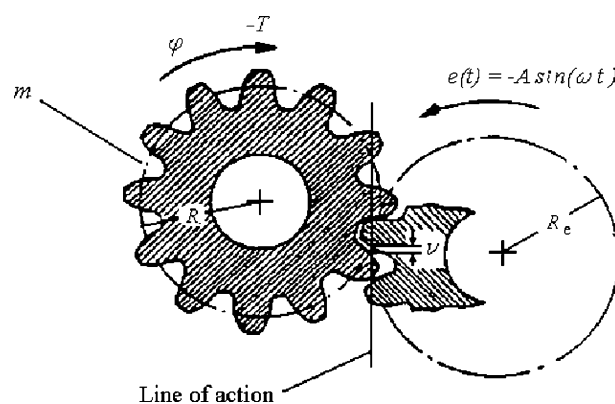
Fig. 1. Schematic view of a single-stage gearbox system.

The driving gear undergoes a harmonic rotational motion with angular amplitude A and frequency ω described by $e(t) = -A\sin(\omega t)$. The relative displacement between the gears due to the backlash is thus

$$s = \frac{AR_e}{v}\sin\omega t - \frac{R}{v}\varphi, \tag{2}$$

in such a way that $-1 < s < 0$.

The equation of motion, in the relative coordinates, is obtained by substituting (2) into (1), what gives

$$\ddot{s} + \beta\dot{s} = \ddot{e} + \beta\dot{e} + \gamma, \tag{3}$$

where dots stand for derivatives with respect to the scaled time $\tau = \omega t$, and we have introduced the following nondimensional parameters

$$\alpha \equiv \frac{AR_e}{v}, \tag{4}$$

$$\beta \equiv \frac{d}{m\omega}, \tag{5}$$

$$\gamma \equiv \frac{TR}{m\omega^2}, \tag{6}$$

representing the damping coefficient, excitation amplitude, and inertias moment, respectively.

Due to its linearity, Eq. (3) can be analytically integrated, between two impacts of the gear teeth, after specification of the initial conditions: $s(\tau_0) = s_0$ and $\dot{s}(\tau_0) = \dot{s}_0$. There results, for the displacement s and velocity $\dot{s}$ between impacts, the following expressions

$$s(\tau) = s_0 + \alpha(\sin\tau - \sin\tau_0) + \frac{\gamma}{\beta}(\tau - \tau_0) + \frac{1}{\beta}\{1 - \exp[-\beta(\tau - \tau_0)]\}\left(\dot{s}_0 - \alpha\cos\tau_0 - \frac{\gamma}{\beta}\right), \tag{7}$$

$$\dot{s}(\tau) = \alpha\cos\tau + \left(\dot{s}_0 - \alpha\cos\tau_0 - \frac{\gamma}{\beta}\right)\exp[-\beta(\tau - \tau_0)] + \frac{\gamma}{\beta}. \tag{8}$$

An impact, on its hand, occurs whenever $s = -1$ or 0, for they correspond to the backlash boundaries. At these points the motion is no longer smooth and we have to reset the initial conditions, according to the laws of inelastic impact:

$$\tau_0 = \tau, \tag{9}$$

$$s_0 = s, \tag{10}$$

$$\dot{s}_0 = -r\dot{s}, \tag{11}$$

where $0 < r < 1$ is the restitution coefficient.

Since there is an analytical solution for the motion between impacts, and each impact implies a simple resetting of the variables, we can work in discrete time, adopting as the time unit the instant of each collision. Accordingly, we will define the discrete variables s_n, $\dot{s}_n$, and τ_n as the displacement, velocity, and time (modulo 2π) just before the nth impact. Substituting the initial conditions $\tau_0 = \tau_n$, $s_0 = s_n$, and $\dot{s}_0 = -r\dot{s}_n$ into Eqs. (7) and (8) we have, for the $n + 1$th impact, the following two-dimensional mapping [13]:

$$s_{n+1} = s_n + \alpha(\sin\tau_{n+1} - \sin\tau_n) + \frac{\gamma}{\beta}(\tau_{n+1} - \tau_n) - \frac{1}{\beta}(1 - \exp[-\beta(\tau_{n+1} - \tau_n)])\left(r\dot{s}_n + \alpha\cos\tau_n + \frac{\gamma}{\beta}\right), \tag{12}$$

$$\dot{s}_{n+1} = \alpha\cos\tau_{n+1} + \frac{\gamma}{\beta} - \exp[-\beta(\tau_{n+1} - \tau_n)]\left(r\dot{s}_n + \alpha\cos\tau_n + \frac{\gamma}{\beta}\right), \tag{13}$$

which is useful when computing Lyapunov exponents, for example.

Fig. 2 shows an example of numerical solution of the gearbox equations (in continuous time) by considering the following set of parameters: $\alpha = 0.5$, $\beta = 0.1$, $\gamma = 0.1$, and $r = 0.9$. In Fig. 2(a) we follow the time evolution of the angle φ (in the absolute coordinate system) of the second gear, represented as the zigzag path, revealing a regular oscillation which follows the regular driving of the first gear. The wiggling lines above and under the zigzag path represents the evolution of the position of the driving wheel, which follows a sinusoidal law. Fig. 2(b) depicts the same situation, but in the relative coordinates, for which the collisions occur at fixed $s = 0, -1$. The possibility of having irregular (actually chaotic) oscillations, is exemplified by Fig. 3(a) and (b), for absolute and relative coordinates, respectively, where the normalized driving amplitude α has been raised to 3.0, the remaining parameters being held constant.
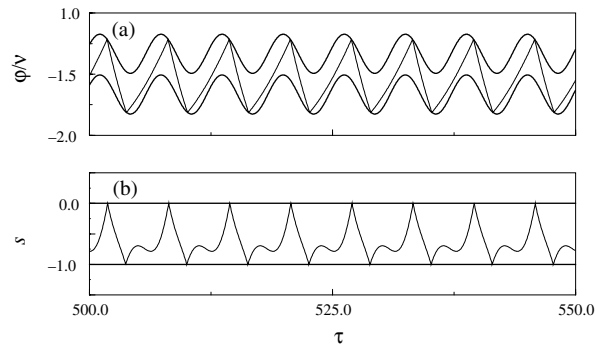
Fig. 2. Time-series of the angular displacement of the second gear in (a) absolute; and (b) relative coordinates. The system parameters were chosen as $\alpha = 0.5$, $\beta = 0.1$, $\gamma = 0.1$ and $r = 0.9$.
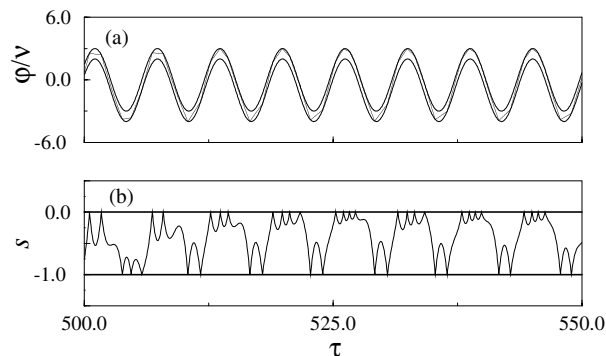
Fig. 3. Time-series of the angular displacement of the second gear in (a) absolute; and (b) relative coordinates. The system parameters were chosen as in the previous figure, except for $\alpha = 3.0$.

3. Crisis and intermittency

The mapping equations are useful for evidencing general dynamical patterns, as shown by the bifurcation diagram of Fig. 4(a), where the asymptotic pattern displayed by the discretized velocity $\dot{s}_n$ is plotted against the restitution coefficient. The companion Fig. 4(b) depicts the Lyapunov exponents corresponding to these asymptotic attractors in the two-dimensional phase-space of $\dot{s}$ and τ. The Lyapunov exponents were computed through $\lambda_i = \lim_{n\to\infty}(1/n)\ln|\Lambda_i(n)|(i = 1, 2)$, where $\Lambda_i(n)$ are the eigenvalues of the matrix $\mathbf{A} = \mathbf{J}_1 \cdot \mathbf{J}_2, \ldots, \mathbf{J}_n$, where $\mathbf{J}_n$ is the Jacobian matrix of the mapping (12) and (13), computed at time n [14].

The case of Fig. 3, for which $r = 0.9$, is clearly seen as a chaotic attractor (the maximal Lyapunov exponent λ_1 is positive), and this behavior persists for smaller values of r, until, at $r = r_2$, the chaotic attractor suddenly jumps into a stable period-1 orbit with six impacts during a cycle corresponding to an entire driving period.

In order to investigate the nature of this transition, we plot in Fig. 5(a) the time-series of the discrete velocities for r slightly higher than the critical value r_2. It shows laminar regions of period-1 (with six impacts *per* period) being interrupted by chaotic bursts in an intermittent fashion. The same conclusion comes from 5(b), where a similar time-series is plotted for a stroboscopic map, which samples the $\dot{s}$ variable after each six collisions. As we move far away from the critical point (Fig. 6), the intermittent bursting becomes more and more frequent, and the duration of the laminar phases tend to zero. This is the typical scenario of type-I intermittency, where, at $r = r_2$, a pair of stable and unstable period-1 orbits are created through a saddle-node bifurcation [19].

As the restitution coefficient is further decreased in the bifurcation diagram of Fig. 4(a), this period-1 orbit apparently undergoes a period-doubling bifurcation cascade which brings about chaotic dynamics for $r \approx 0.75$ in six disjoint bands. These bands suddenly merge into a single chaotic band at $r = r_1$, and this new chaotic regime persists for smaller r, with periodic windows, as can be checked in the fluctuations experienced by the Lyapunov exponent (Fig.
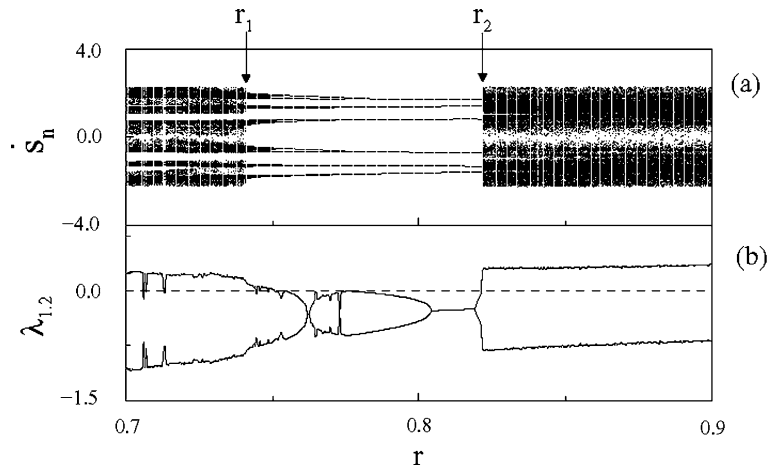
Fig. 4. (a) Bifurcation diagram for the discrete velocity of the second gear, as a function of the restitution parameter. The values of the remaining parameters are $\alpha = 3.0$, $\beta = 0.1$, $\gamma = 0.1$. (b) Lyapunov exponents. The arrows indicate the points where there occurs a crisis (r_1) and intermittency (r_2).
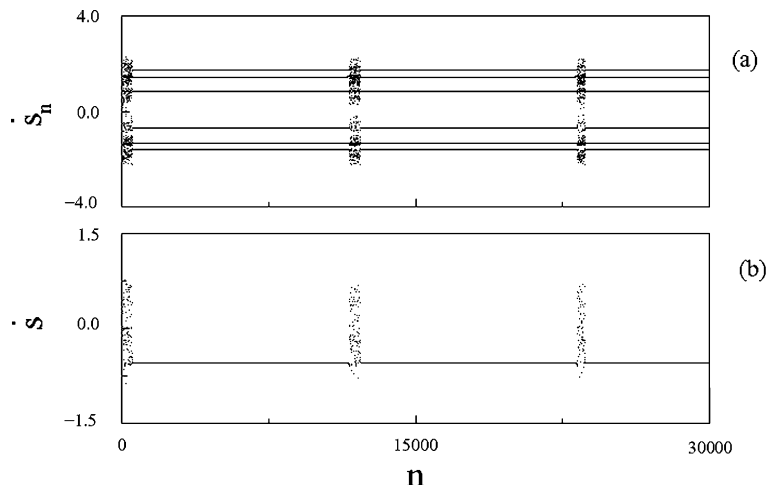
Fig. 5. (a) Time-series of the discrete velocity $\dot{s}_n$ of the second gear, for $\alpha = 3.0$ and $r = 0.82144 \gtrsim r_2$; (b) same figure for the velocity $\dot{s}$ sampled at time intervals $t_n = (2\pi/\omega)n$, with $n = 0, 1, 2, \ldots$.

4(b)). This transition is now due to an interior crisis event, where the chaotic bands existing for $r > r_1$ collide, at $r = r_1$ with the unstable period-1 orbit which was created at the saddle-node bifurcation in $r = r_2$ [19].

Just after the crisis has occurred, at $r < r_1$, although the chaotic trajectories move in a single band, they keep some memory of the bands in they have been confined before the crisis. Hence, the post-critical scenario is typically an intermittent jumping between chaotic motion in bands, as depicted in Fig. 7(a) and (b), where both the Poincaré and stroboscopic maps show this kind of behavior.

4. Riddled-like basins of transient chaos

When a dynamical system presents more than one attractor, we are often interested in knowing to which one a given initial condition asymptotes to. The set of initial conditions in phase space which asymptotes to a given attractor is its basin of attraction. This notion can be extended to behaviors more general that a stationary attracting state, as evidenced by numerical experiments on chaotic scattering, where the trajectories enter into a scattering region and exit
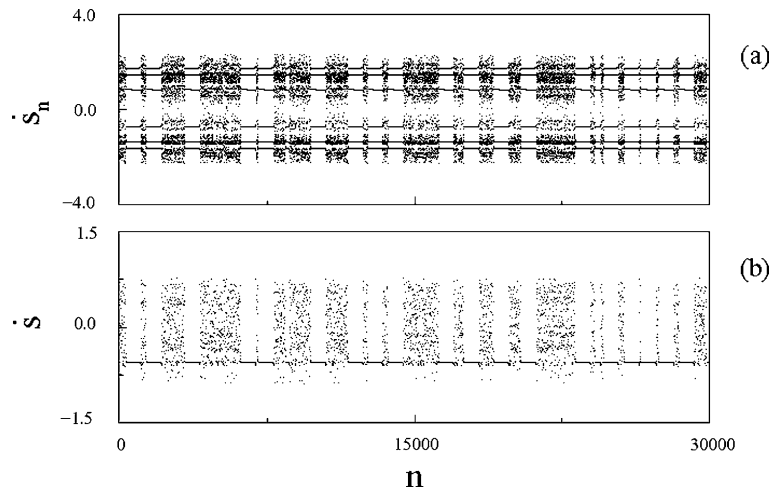
Fig. 6. (a) Time-series of the discrete velocity $\dot{s}_n$ of the second gear, for $\alpha = 3.0$ and $r = 0.82145 \gtrsim r_2$; (b) same figure for the velocity $\dot{s}$ sampled at time intervals $t_n = (2\pi/\omega)n$, with $n = 0, 1, 2, \ldots$.
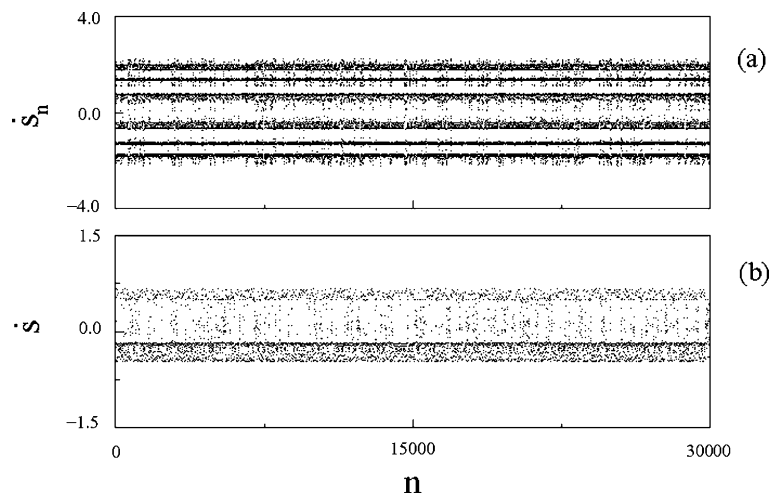
Fig. 7. (a) Time-series of the discrete velocity $\dot{s}_n$ of the second gear, for $\alpha = 3.0$ and $r = 0.74001 \lesssim r_1$; (b) same figure for the velocity $\dot{s}$ sampled at time intervals $t_n = (2\pi/\omega)n$, with $n = 0, 1, 2, \ldots$.

through one or more possible ways. The exit basin is thus defined as the set of initial conditions which lead to open trajectories which escape through a given exit [20]. These trajectories, on their hand, are not chaotic orbits, strictly speaking, but rather chaotic transients. For example, if the scattering region is comprised of three circular disks, a trajectory will typically spend some time bouncing around these disks in an erratic fashion before escaping to infinity through one of the three exits of the open system [21]. The exit basin of this problem possesses, besides a fractal geometry for its boundary, the even more restrictive property of Wada: a circle centered at any point of the boundary intercepts basins of all attractors (three or more of them) [22].

In a more general context, we can speak of basins of transient chaos, as the set of initial conditions which lead to chaotic transients with some desired property. This idea has been used to identify transient basins of magnetic field lines in tokamaks which hit the vessel wall in pre-specified regions [23]. For the gear-rattling problem, we have observed the existence of chaotic transients associated with crises, as mentioned in the previous section.

In Fig. 8(a), for example, we identify the occurrence of a crisis in the bifurcation diagram for the discrete velocity of the second gear, when the varying parameter is the excitation amplitude α of the driving gear, the restitution coefficient being kept constant. At the critical value $\alpha_1 \approx 1.24370$ there occurs a crisis, since the chaotic attractor existing before α_1
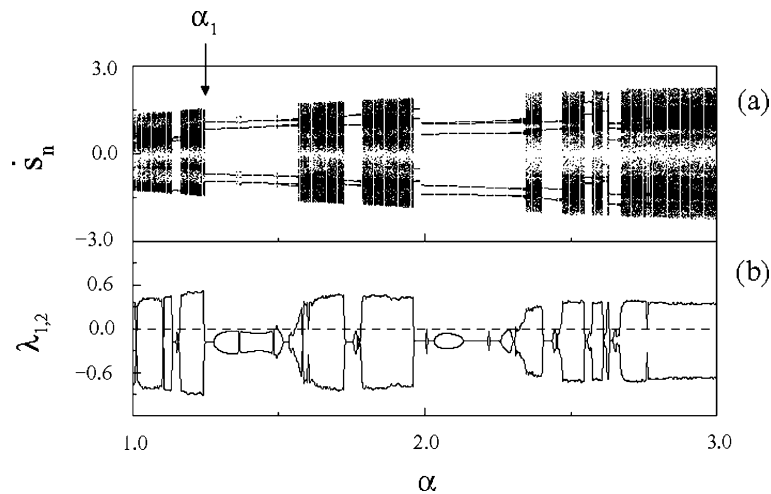
Fig. 8. (a) Bifurcation diagram for the discrete velocity of the second gear, as a function of the excitation amplitude. The values of the remaining parameters are $r = 0.9$, $\beta = 0.1$, $\gamma = 0.1$. (b) Lyapunov exponents.

(see the corresponding Lyapunov exponents in Fig. 8(b)) suddenly disappears, and a stable period-1 orbit (with four impacts per period) emerges out. For α just after α_1, the motion initially is a chaotic transient which eventually asymptotes to this stable orbit.

The chaotic transient appears because, after the crisis has been occurred, the formerly attracting chaotic set becomes a nonattracting chaotic saddle. This saddle has essentially the same complicated structure of homoclinic and hetero-clinic crossings between invariant manifolds, such that an orbit which enters this saddle will experience a motion with similar characteristics to that it would have in a chaotic attractor. Hence, for a finite time, the chaotic transient resembles the orbit it would have in the pre-critical attractor [17].

Hence, different initial conditions will produce chaotic transients with a correspondingly distinct duration. We will define a transient basin as the set of initial conditions which produce a chaotic transient whose duration is within a given interval. In Fig. 9 we plot numerical approximations of transient basins related to a situation in which the excitation amplitude is slightly higher than the crisis value α_1 of Fig. 8. We plot with black pixels those initial conditions which lead to transients of duration less than a given integer value n, and the pixed is left blank otherwise. We will refer to the black and white regions as the basins of "short" and "long" transients, respectively. The distribution of black and white points evidently depends on the value of n we have specified.

For example, if we choose a small value of n, say, 90 (Fig. 9(a)), the basin of "fast" transients is the union of well-defined tongues with inclusive fingers. The majority of initial conditions is in the basin of "long" transients. If we increase progressively the value of n (Fig. 9(b)–(d)), the white region of long transients becomes filled with black points. The more we wait to set a chaotic transient duration n, more points will be considered as "fast" ones. In the limit of n going to infinity, almost all points (with the exception of a measure zero set of points exactly on the chaotic saddle) will eventually go to the attractor, and the black basin would essentially include all the available phase space area.

There are regions in Fig. 9 in which the transient basins are so densely intermixed that there seems that any point belonging to some basin has a neighborhood containing points belonging to the other basin. As this neighborhood may stand, for example, for the experimental uncertainty in the determination of the initial condition, the existence of neighborhoods with arbitrarily small radius, and which contain points belonging to other basins, is a troublesome situation. In order to numerically check this claims, we have selected a box within a densely mixed part of Fig. 9 with initial conditions $3.0 < \tau_0 < 3.5$ and $0 < \dot{s}_0 < 0.5$, and choose randomly a large number, say 3000, points. For each initial condition A: $(\tau_0, \dot{s}_0)$ so chosen, we keep $\dot{s}_0$ constant and vary the other coordinate by a small amount ϵ. This procedure is equivalent to choose, besides A, also the slightly displaced initial conditions: B: $(\tau_0 + \epsilon, \dot{s}_0)$ and C: $(\tau_0 - \epsilon, \dot{s}_0)$.

If the transient orbit starting from initial condition A goes to one of the transient basins, and either one (or both) of the displaced initial conditions, B or C, go to the other basin, we call A as an ϵ-uncertain initial condition. By considering a large number of such points, we can estimate the fraction of ϵ-uncertain points in the box, $f(\epsilon)$. This number scales with the uncertain radius as a power-law $f(\epsilon) \sim \epsilon^\varpi$. where ϖ is called uncertainty exponent [24]. Since the underlying phase space is two-dimensional, it turns out that the box-counting dimension of the boundary between
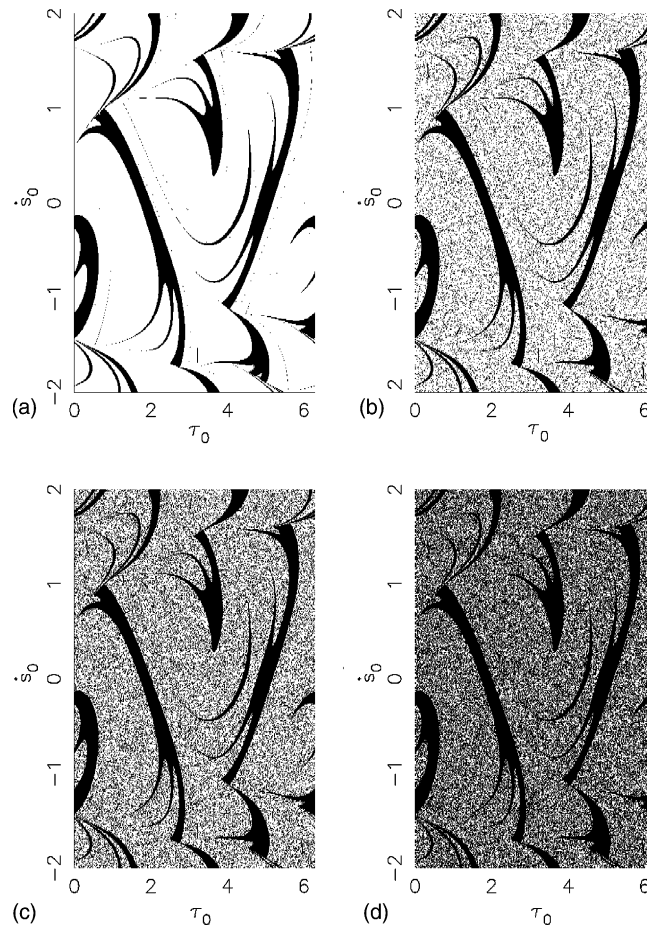
Fig. 9. Basins of transient motion for $\alpha = 1.24500 \gtrsim \alpha_1$ for (a) $n = 90$; (b) $n = 500$; (c) $n = 1000$; and (d) $n = 2000$.

transient basins is $D = 2 - \varpi$. If $\varpi = 1$, i.e., the uncertain fraction scales linearly with the uncertain radius, it follows that the basin boundary is a smooth curve, since $D = 1$.

On the other hand, if $0 < \varpi < 1$, the basin boundary has a fractal dimension between 1 and 2. The limiting case, $\varpi = 0$, is such that the uncertain fraction is constant regardless of how small the uncertainty ϵ may be. This reflects an extreme sensitivity to the initial condition, since there is essentially no way of improving the knowledge about the transient behavior starting from one initial condition. Viewed from a geometrical perspective, the basin boundary dimension is equal to the phase space dimension, in such a way that the basins are so intermixed that their boundary fills up the available space, what really seems to occur in regions of Fig. 9(b)–(d).

This is a characteristic feature of riddled basins of attraction, for which the basin is punctured (in an arbitrarily fine scale) with holes belonging to the basin of another attractor. However, the mathematical conditions for the existence of riddled basins are too restrictive to be fulfilled in real engineering systems, so that the concept of practically riddled basins has been proposed [25,26]. The extension of such riddled-like basins, with a vanishing uncertainty exponent, to transient basins, has been made recently [27].

Fig. 10 shows numerical results for the uncertain fraction by considering a box picked up from situations where the transient basins are apparently riddled-like. Squares are for a transient duration of $n = 500$, whereas filled circles were obtained for $n = 1000$. The uncertainty exponents were obtained as $\varpi = 0.010 \pm 0.001$ and 0.003 ± 0.002 for these two cases, respectively. Within the numerical accuracy, we claim that, if the transient basins are not riddled-like, they are at least extremely densely intertwined (the corresponding dimension of the basin boundary is nearly of the phase space). This is, from the practical point of view, indistinguishable of actual riddling.

The duration of the transients is strongly dependent on the initial condition chosen. In order to investigate the statistical distribution of the transient durations, we have picked up a box in the $\tau_0 \times \dot{s}_0$ plane, with coordinates
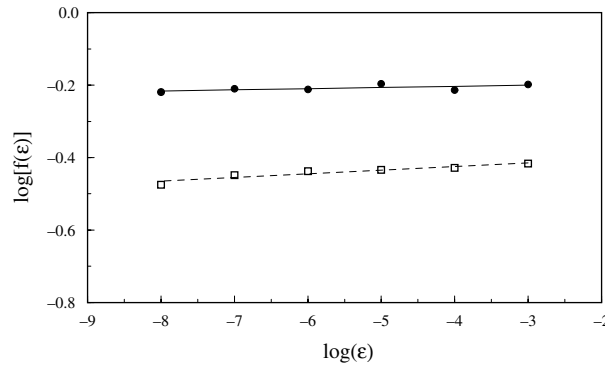
Fig. 10. Fraction of uncertain initial conditions for transient orbits with duration less than $n = 500$ (squares) and $n = 1000$ (filled circles). The straight lines are least squares fits.
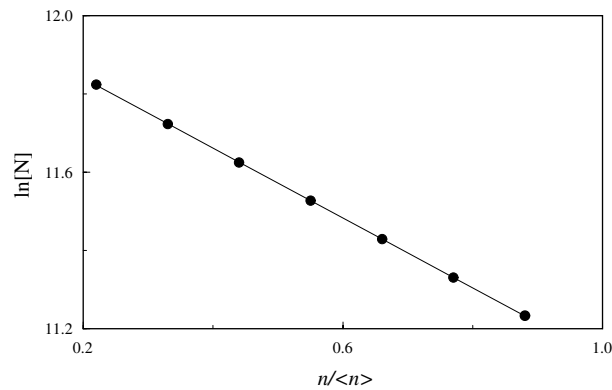
Fig. 11. Statistical distribution of the number of transients with duration less than n iterations. The straight line corresponds to the fit given by Eq. (14).

$0 < \dot{s}_0 < 0.5$ and $3.0 < \tau_0 < 3.5$, and cover it with a mesh of 400×400 initial conditions. Each initial condition was iterated n times before we checked whether or not the transient has decayed to an attractor. We denote by $N(n)$ the number of initial conditions which generate orbits which do not go to the corresponding attractor after n iterations, i.e., we compute the orbits which remain as transients.

We have observed (Fig. 11) an exponential distribution for the number of transients with duration less than n iterations:

$$N(n) = N_0 \exp\left(-\kappa \frac{n}{\langle n \rangle}\right), \tag{14}$$

where $\langle n \rangle = 2272$ is the average transient duration, and slope $\kappa = 0.893 \pm 0.001$. The exponential distribution of transient times is a general characteristic of dynamical systems after a crisis, for which the former chaotic attractor has been replaced by a nonattracting chaotic saddle [17].

5. Conclusions

Let us conclude this article by mentioning some practical implications of our results in the modeling of gearboxes. While some unwanted effects of rattling are normally related to irregular, or chaotic impacts occurring in this system, the intermittent transition chaos–order may be regarded as a kind of control of rattling through the increase of dissipation in the impacts between gear teeth, or the decrease of the restitution coefficient. Suppression of chaos through augmenting dissipation is a well-known solution in vibration engineering [18].

We have found sudden changes in chaotic attractors which have a very complicated structure of transient basins, for which the boundary seems to be so involved that the duration of the corresponding chaotic transient presents extreme sensitivity to the initial state. On the other hand, the sudden expansion in the chaotic attractor through a crisis may cause an unwanted increase in the rattling even though we are increasing dissipation. This shows that a naive approach based only on increase of the friction may not lead to the desired result of suppressing rattling, and a more profound analysis is necessary. This was the main motivation of the present paper.

Acknowledgements

References

[1] Kapitaniak T. Chaos for engineers. New York, Berlin, Heidelberg: Springer; 2000.
[2] Wiercigroch M, DeKraker B. Applied nonlinear dynamics and chaos of mechanical systems with discontinuities. Singapore: World Scientific; 2000.
[3] Thompson JMT. Global dynamics of oscillations: fractal basins and intermediate bifurcations. In: Aston PJ, editor. Nonlinear mathematics and its applications. Cambridge: Cambridge University Press; 1996.
[4] Nordmark AB. Non-periodic motion caused by grazing in an impact oscillator. J Sound Vib 1991;145:279–97.
[5] Dankowicz H, Piiroinen P, Nordmark AB. Low-velocity impacts of quasi-periodic oscillations. Chaos, Solitons & Fractals 2002;14:241–55.
[6] Jerrelind J, Stensson A. Nonlinear dynamics of parts in engineering systems. Chaos, Solitons & Fractals 2000;11:2413–28.
[7] Pfeiffer F. Seltsame Attraktoren in Zahnradgetrieben. Ing Arch 1988;58:113–25.
[8] Karagiannis K, Pfeiffer F. Theoretical and experimental investigations of gear-rattling. Nonlinear Dyn 1991;2:367–87.
[9] Hongler M-O, Streit L. On the origin of chaos in gearbox models. Physica D 1988;29:402–8.
[10] Blazejczyk-Okolewska B, Czolczynski K, Kapitaniak T, Wojewoda J. Chaotic mechanics in systems with friction and impacts. Singapore: World Scientific; 1999.
[11] Blazejczyk-Okolewska B, Kapitaniak T. Coexisting attractors of impact oscillator. Chaos, Solitons & Fractals 1998;9:1321–38.
[12] Pfeiffer F, Kunert A. Rattling models from deterministic to stochastic processes. Nonlinear Dyn 1990;1:63–74.
[13] de Souza SLT, Caldas IL. Basins of attraction and transient chaos in a gear-rattling model. J Vib Control 2001;7:849–62.
[14] de Souza SLT, Caldas IL. Calculation of Lyapunov exponents in systems with impacts. Chaos, Solitons & Fractals 2004;19:569–79.
[15] de Souza SLT, Caldas IL. Controlling chaotic orbits in mechanical systems with impacts. Chaos, Solitons & Fractals 2004;19:171–8.
[16] de Souza SLT, Caldas IL, Balthazar JM, Brasil RMLRF. Analysis of regular and irregular dynamics of a non ideal gear rattling problem. J Brazil Soc Mech Sci 2002;XXIV:111–4.
[17] Grebogi C, Ott E, Yorke JA. Crises, sudden changes in chaotic attractors, and transient chaos. Physica D 1983;7:181.
[18] Moon FC. Applied dynamics with applications to multibody and mechatronic systems. New York: John Wiley; 1998.
[19] Ott E. Chaos in dynamical systems. Cambridge: Cambridge University Press; 1993.
[20] Ding M, Grebogi C, Ott E, Yorke JA. Transition to chaotic scattering. Phys Rev A 1990;42:7025–40.
[21] Bleher S, Grebogi C, Ott E. Bifurcation of chaotic scattering. Physica D 1990;46:87–121.
[22] Poon L, Campos J, Ott E, Grebogi C. Wada basin boundaries in chaotic scattering. Int J Bifurcat Chaos 1996;6:251–65.
[23] da Silva EC, Caldas IL, Viana RL, Sanjuan M. Escape patterns, magnetic footprints, and homoclinic tangles due to ergodic magnetic limiters. Phys Plasmas 2002;9:4917.
[24] Grebogi C, Ott E, Yorke JA. Fractal basin boundaries. Physica D 1983;17:125–53.
[25] Blazejczyk-Okolewska B, Brindley J, Kapitaniak T. Practical riddling. Chaos, Solitons & Fractals 2000;11:2511.
[26] Kapitaniak T. Partially nearly riddled basins in systems with chaotic saddle. Chaos, Solitons & Fractals 2001;12:2363–7.
[27] Woltering M, Markus M. Riddled-like basins of transient chaos. Phys Rev Lett 2000;84:630–4.